Helium nanodroplet infrared spectroscopic studies of CH_4^+ and $^{13}CH_3^+$

Amandeep Singh [1], Sofia H. Allison[1,2], Andrew Abhisek A. Azhagesan[1,3], and Andrey F. Vilesov[1,4,]*

[1] Department of Chemistry, University of Southern California, Los Angeles, CA, 90089, USA

[2] Mount St. Mary's University, Emmitsburg, MD, 21727, USA

[3] Department of Computer Science, University of Southern California, Los Angeles, CA, 90089, USA

[4] Department of Physics and Astronomy, University of Southern California, Los Angeles, CA, 90089, USA

[*] Author to whom correspondence should be addressed.

Electronic address: vilesov@usc.edu

~~Contact~~ Phone number: 1(213)8212936

Abstract

In this work, CH_4^+ cations were formed in helium droplets and investigated with infrared laser spectroscopy. The observed infrared bands are assigned to the C_{2v} isomer of the CH_4^+ cation. The rotational structure of the bands remains unresolved indicating a factor of three or larger decrease in the rotational constants in helium nanodroplets. We also report on the observation of the spectrum of isotopically substituted $^{13}CH_3^+$ cations in He droplets which shows well-resolved rotational structure. The rotational constant A for rotation about the C_3 axis of CH_3^+ in helium was found to be a factor of 1.17 smaller than in the gas phase.

Introduction

Methane is the simplest hydrocarbon molecule, but its cationic counterpart is rarely explored spectroscopically. The vertical ionization of methane forms a hypothetical CH_4^+ cation in a triply degenerate T_2 electronic state prone to $T\times(t_2+e)$ Jahn-Teller distortion. [1-3] CH_4^+ ions can undergo linear Jahn-Teller distortion to form local minimum structures such as D_{2d} or a $C_{3v,}$ whereas the quadratic distortion leads to a C_{2v} symmetric geometry. [1-4] There are 12 equivalent C_{2v}, 8 equivalent C_{3v}, and 6 equivalent D_{2d} potential minima structures on the PES (Potential Energy Surface) of CH_4^+. [5] The low-lying transition states ensure tunneling among the different isomers of CH_4^+. [6] Theoretical calculations predict the global minimum C_{2v} structure with two long CH bonds and two short CH bonds, [2, 3, 5, 7-11] along with local minimum C_{3v} and D_{2d} isomers. A variety of spectroscopic techniques such as photoelectron spectroscopy, [12, 13] PFI-ZEKE photoelectron spectroscopy, [14, 15] and ESR spectroscopy in cold neon matrices [16, 17] were used to verify the C_{2v} geometry of CH_4^+ ions as the ground state. Signorell et al. reported the rotationally resolved spectra of CH_4^+ [14, 15] and $CD_2H_2^+$ [18] using ZEKE (Zero Kinetic Energy) spectroscopy. However, the results of Coulomb explosion experiments [19, 20] indicated the C_{2v} geometry as a saddle point on PES and show that the cation undergoes a pseudo rotation among the equivalent structures.

Lowering the temperature of a system is a proven way to investigate highly reactive molecules and ions. Recently, Davies et al. reported the infrared spectrum of CH_4^+ cations solvated in small helium clusters (CH_4^+-He_N; N<100) at T~5K. [21] The spectrum shows two broad infrared bands in the CH stretching region at 3044 cm^{-1} and 3149 cm^{-1} which the authors assigned to the symmetric and antisymmetric CH stretches of the short CH bonds in the C_{2v} geometry. [21] The

spectra in small He clusters could have some inhomogeneous broadening due to the cluster size distribution.

In this work, large helium nanodroplets of about 10^4 atoms are used as hosts for CH_4^+ cations. Nanodroplets have a lower temperature of about 0.4 K and are large enough to fully surround small cations such as CH_4^+ with multiple solvation shells to create a more homogeneous environment than in small clusters. The large ionization potential of helium atoms and superfluidity at low temperatures make helium nanodroplets ideal soft matrices for molecular cations. [22-27] Here we report the infrared spectrum of the CH_4^+ cations at better resolution compared with previous measurements confirming the C_{2v} geometry of the CH_4^+ cation. We also report on the observation of the spectrum of isotopically substituted $^{13}CH_3^+$ cations, which show a well-resolved rotational structure. The obtained rotational constants for $^{13}CH_3^+$ are similar to those previously reported for $^{12}CH_3^+$ solvated in helium droplets. [27] The mechanism of the formation of cations is elucidated by measuring the dependence of infrared bands' intensity versus the methane pressure in the pickup chamber.

Experimental Methods

The experimental setup is described in detail elsewhere.[28] Superfluid helium droplets are produced by the pulsed expansion of helium gas into a vacuum chamber at a stagnation pressure of 23 bar at a temperature of 23 K. The droplets pass through a skimmer and are doped with 99.99 % pure methane (containing nominal 1.3-1.8% $^{13}CH_4$) molecules in the 44 cm long pickup chamber. Further downstream the droplets are ionized by electron impact (100 eV) and traverse through an RF octupole ion guide collision cell filled with helium gas at ~10^{-5} mbar. The collisions with helium atoms in the cell reduce the droplets' size, which greatly increases the magnitude of the laser-induced signal. The droplets interact with a pulsed laser beam while they pass through the ion region of the quadrupole mass spectrometer (QMS). Vibrational excitation of ions leads to the evaporation of He atoms from the droplet and liberation of free ions which are then mass-filtered by a QMS. The mass-selected ions are detected by a Channeltron electron multiplier. The signal from the electron multiplier is amplified by an SR570 current amplifier and recorded using an SR250 boxcar integrator with ~3μs gate width.

This work employed an OPO/OPA laser system by LaserVision with a nominal spectral linewidth of ~1 cm^{-1}, a repetition rate of 20 Hz, and a pulse width of 7 ns. The laser is calibrated by recording the rovibrational spectrum of HCl, CD_4, and CH_4 in an optoacoustic cell.

Results

The series of experiments started with measuring the mass spectrum of methane-doped helium droplets upon electron impact ionization, which is shown in Fig. 1. The ionization of doped droplets produces a variety of cations such as CH_3^+, CH_4^+, CH_5^+, $(CH_4)_2^+$, etc.. The focus of this work is the spectroscopy of CH_4^+ and $^{13}CH_3^+$ cations. The spectra of CH_3^+, CH_5^+, and CDH_4^+ cations are reported in ref. [27, 29]. The results on the infrared spectra of other ions will be presented elsewhere.

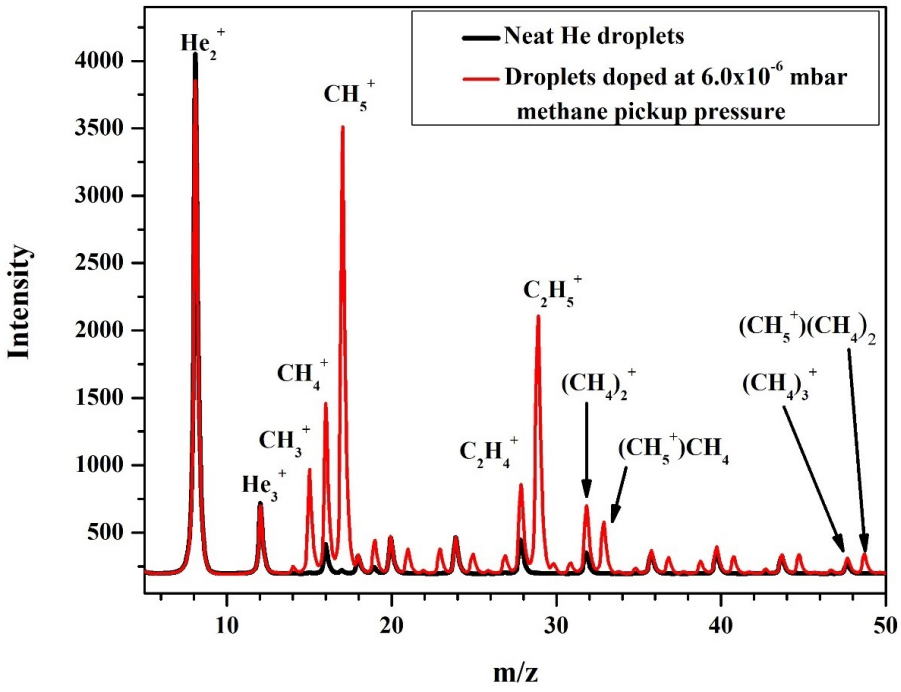

Figure 1: The mass spectrum of the ions liberated from neat helium droplets (black trace) and from the helium droplets doped with methane (red trace) at 6.0×10^{-6} mbar pickup pressure measured upon the electron impact ionization.

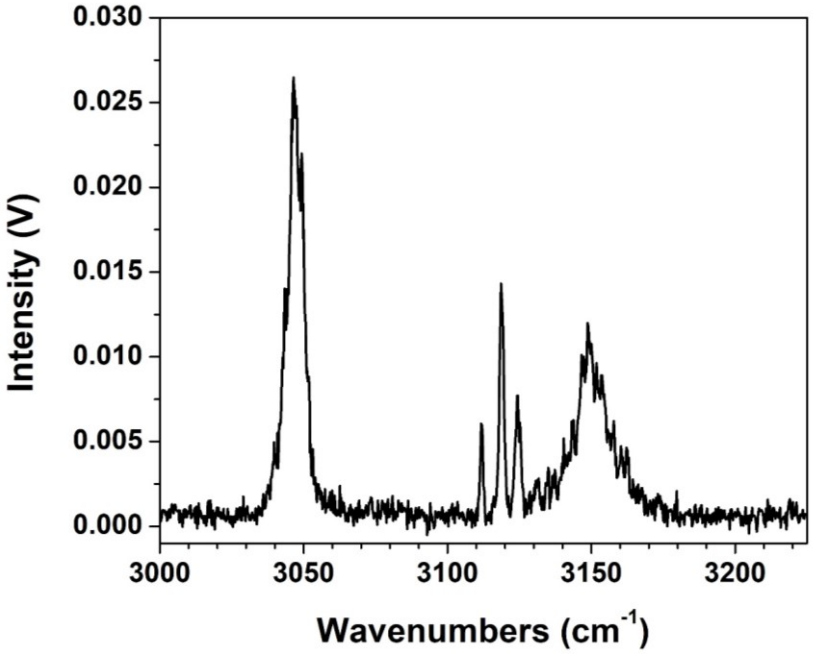

Figure 2: The mass-selected infrared spectrum measured at m/z = 16 mass channel by maintaining the pickup pressure of methane 1.2x10^{-6} mbar.

Figure 2 shows the infrared spectrum in the range of 3000 to 3225 cm^{-1} measured at mass channel m/z = 16 by maintaining 1.2×10^{-6} mbar pickup pressure of methane. The RF octupole collision cell was filled with 1.0×10^{-5} mbar of helium gas. Here and later, the pressures of gases reported are the nominal readings from the ion gauge controllers. The absolute pressure of gases could be obtained by dividing the nominal reading by 1.40 for methane and 0.18 for helium gas. Figure 2 shows two broad infrared bands with maxima at 3047 cm^{-1} and 3149 cm^{-1} having widths of 7 and 16 cm^{-1} (FWHM), respectively. The spectra measured at different pickup pressure of methane from 0.6×10^{-5} to 2×10^{-5} mbar (not included here) show the same relative intensity of the bands. Similar but broader (~50 cm^{-1}) bands were previously observed for CH_4^+ ions solvated in

small He clusters, which were assigned to the stretching modes of the CH_4^+ ions with C_{2v} structure. [21] In addition, the spectrum in Fig. 2 has a new band which appears as a triplet of narrow (FWHM ~ 1.5 cm^{-1}) peaks with the central peak centered at 3118.6 cm^{-1}. This new band may have been also been contributing to the previous lower resolution spectrum which shows a broad shoulder extending in the range of 3100-3150 cm^{-1}. [21] No other features were found in the lower frequency range from 2500-3000 cm^{-1}.

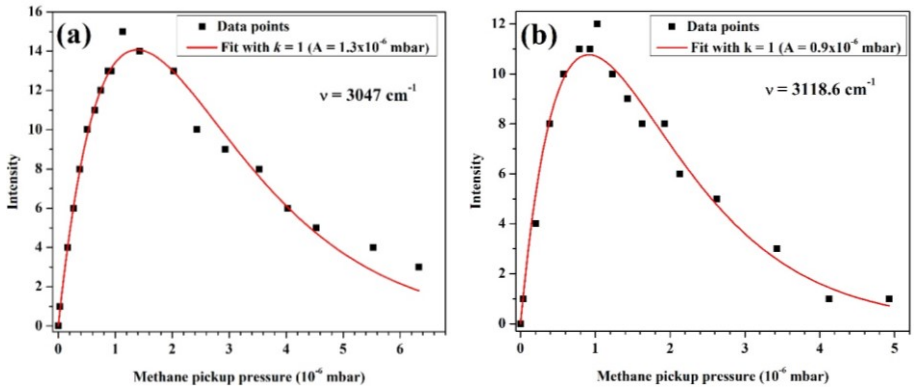

Figure 3: The methane pickup pressure dependence on the intensity of infrared bands at 3047 cm^{-1} (a) and 3118.6 cm^{-1} (b). The data points are fitted with a Poisson distribution equation (red traces) as described in the text.

Figure 3 shows the methane pickup pressure dependence on the intensity of the infrared bands at 3047 cm^{-1} (Figure 3a) and 3118.6 cm^{-1} (Figure 3b). The red trace shows the fitting with the Poisson equation for capturing a single methane molecule:

$$I(P) = C \cdot (P/A) \cdot e^{-\frac{P}{A}} \qquad \text{(Eq. 1)}$$

Here, P is the pickup pressure. The fitting constant 'A' gives the pickup pressure of methane, at which the greatest number of droplets are doped with a single methane molecule, and 'C' is the proportionality constant. Good agreement between the experimental results and the fits signifies that both infrared bands stem from ionizing the droplets doped with a single methane molecule. However, the intensity of the band at 3047 cm^{-1} maximizes at a higher pickup pressure of methane (1.3×10^{-6} mbar) compared to the band at 3118.6 cm^{-1} (0.9×10^{-6} mbar). Different pickup pressure dependence indicates that the two bands belong to different cations.

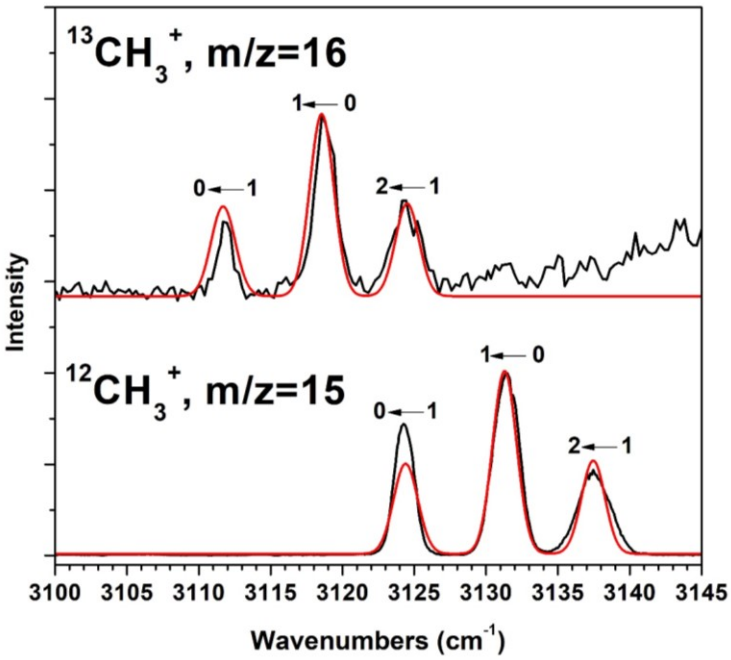

Figure 4: The comparison of the infrared spectrum of $^{12}CH_3^+$ cations measured at m/z=15 , and the zoomed-in infrared spectrum measured in this work at m/z=16 . The black traces show the experimentally measured spectra and the red traces show the simulated spectra for the $^{12}CH_3^+$ and $^{13}CH_3^+$ cations, respectively. See the text for more details.

Figure 4 shows the infrared spectra of $^{12}CH_3^+$ ions obtained in this work (solid black trace in lower panel) measured by maintaining 7.0×10^{-7} mbar pressure of methane in the pickup chamber and 1.0×10^{-5} mbar of helium in the octupole at m/z=15 mass channel. The spectrum of $^{12}CH_3^+$ shows three sharp peaks which were assigned to the rovibrational structure similar to that in refs. [21, 27]. The solid black trace in upper panel of Fig. 4 shows the zoomed-in spectrum measured at m/z=16 mass channel, same as in Figure 2. The bands present in the upper panel are assigned to the $^{13}CH_3^+$ ions as will be discussed in the following.

Discussion

The methane-doped droplets are ionized via electron impact. Although the ionization cross-section of a methane molecule is bigger than that of a helium atom, there are ~10^4 He atoms per droplet, leading to an overwhelming probability for the ionization of the He atoms in the droplet. [30, 31] Therefore electron impact first produces He^+ ions which then create the molecular ions via charge transfer.[32]

The removal of an electron from CH_4 produces a triply degenerate electronic state which is subjective to a T×(T+e) Jahn-Teller distortion. [1, 2] The quadratic Jahn-Teller distortion equilibrates the cation in C_{2v} geometry. [1, 2, 4] There are 12 equivalent C_{2v} geometries, 8 equivalent C_{3v} geometries, and 6 D_{2d} geometries on the PES of CH_4^+ present as stationary points.[5] The calculations predict a C_{2v} symmetric geometrical isomer as the global minimum state, which is in agreement with spectroscopic observations. [2, 10, 16, 17, 33, 34] The equilibrium C_{2v} structure of CH_4^+ has two shorter (stronger) CH bonds and two longer (weaker) CH bonds. The spectrum of CH_4^+ solvated in small helium clusters shows two infrared bands in the CH stretching region (3044 cm^{-1} and 3145 cm^{-1}) which were assigned to the C_{2v} structure of CH_4^+. [21] Similarly, we assigned the band at 3149 cm^{-1} to the asymmetric stretching, and the band at 3047 cm^{-1} is assigned to the symmetric stretching of the stronger CH_2 unit. The spectrum did not show any additional bands, which may indicate the absence of the other isomers of CH_4^+ cations. The nominal spectral linewidth of the laser used in this work is ~1 cm^{-1}. In Figure 2, the width of the band of $^{13}CH_3^+$ at 3118.6 cm^{-1} is ~1.5 cm^{-1} (FWHM) but the bands due to CH_4^+ at 3047 cm^{-1} ($\delta\nu \sim 7$ cm^{-1}) and 3149 cm^{-1} ($\delta\nu \sim 16$ cm^{-1}) have significantly larger widths.

The pulse field ionization (PFI) zero kinetic energy (ZEKE) photoelectron spectrum measured with a resolution of ~0.7 cm^{-1} confirms the fluxional nature of the CH_4^+ cation and its

deuterated analogs. [35] Woerner et al. reported that the gas phase rotational constants of the C_{2v} symmetric CH_4^+ in the ground vibrational state to be A=6.40 cm^{-1}, B=5.55 cm^{-1}, C=4.03 cm^{-1}, and the rotational energy levels show splitting of δ =16.4 cm^{-1} due to the tunneling motion of H-atoms between equivalent configurations. [9, 14, 15, 36] CH_4^+ ions have three nuclear spin isomers with nuclear spin symmetries that correlate to A_1 (I=2), E (I=0), and F_2 (I=1) in methane molecules. In CH_4^+ the lowest rotational states of each nuclear spin isomer are *N*=1, 0, and 1, respectively. The population of nuclear spin isomers in He droplets in CH_4 molecules is 5:9:2, respectively. [37] Assuming that the nuclear spin does not relax within the experimental time of about ~0.5 ms, as previously observed in the case of many neutral molecules and ions, [24, 27, 37] the populations of N=0 and N=1 levels are expected to be in the ratio of 9:7. Assuming the same rotational constants for CH_4^+ in the gas phase and the helium nanodroplets, the splitting of the rotational lines should be of the order of 10 cm^{-1}. Figure 2 shows that the symmetric band at 3047 cm^{-1} has an FWHM of $\delta\nu$ ~ 7 cm^{-1} and does not show any rotational structure. Similarly, the broader ($\delta\nu$ ~ 16 cm^{-1}) asymmetric stretching band at 3149 cm^{-1} appears to be devoid of the rotational structure. We conclude that the effective rotational constants of the CH_4^+ ions in He are at least a factor of three smaller than in the gas phase so that the rotational structure fits within the unresolved band contours. In general, the rotational contour of the antisymmetric band is expected to be broader than that of the symmetric band due to different selection rules for the rovibrational transitions, which agree with the observations.

The triplet structure of the band at 3118.6 cm^{-1} appears similar to that observed previously in the spectrum of $^{12}CH_3^+$ centered at 3131.6 cm^{-1} where it was assigned to the rovibrational band associated with the perpendicular asymmetric ν_3 mode.[27] The new band with a triplet structure observed in this work centered at 3118.6 cm^{-1} is assigned to the $^{13}CH_3^+$. The CH_3^+ (D_{3h}) cations

have a symmetric top structure and follow the Fermi-Dirac nuclear spin statistics due to the presence of H atoms. Therefore, at ultralow temperatures, the ions relax into the K=0 and K=1 states which belong to different nuclear spin species and are expected to have equal populations in He droplets. The central band at 3131.6 cm^{-1} is assigned to the K'=1 ← K''=0 transitions of the ν_3 (e←a_1) band whereas the J-structure of the sub-band remains unresolved. [27] The low-frequency sub-band at 3124.7 cm^{-1} is assigned to the K'=0 ← K''=1 transitions and the higher frequency band at 3137.6 cm^{-1} belongs to the K'=2 ← K''=1 transitions. The central sub-band is about a factor of two stronger than the sidebands which have similar intensities that are in agreement with the expected equal population of the K=0 and K=1 states. The distance between the peaks gives the rotational constant 'A' of the CH_3^+, whereas the 'B' constant is small and cannot be determined accurately. The red trace in panel (a) of Fig. 4 shows the simulated spectrum of $^{12}CH_3^+$ cations with modified rotational constants which are listed in Table 1. The band origin of the $^{12}CH_3^+$ ions in He was found to have a high frequency shift by ~20 cm^{-1} as compared to the free ions.

The red trace in Fig. 4 (b) shows the simulated spectrum of $^{13}CH_3^+$ cations with modified rotational constants, (see Table 1). The rotational constant 'A' appears to be the same for both isotopes in He droplets, which agrees with the rotors' geometry. The υ_3 band origin for the $^{13}CH_3^+$ ions has ~12.7 cm^{-1} lower frequency than that for the $^{12}CH_3^+$ ions in this work. This shift is the same as measured for the ions in the gas phase, [38], which supports the assignment of the band in Fig. 4(b) to the $^{13}CH_3^+$ isotopologues.

The rotational constants for both isotopologues of CH_3^+ in the gas phase were obtained to be B (~4.0 cm^{-1}) and A (~9.3 cm^{-1}). [38] However, Table 1 shows that the rotational constants differ significantly for both cations in the gas phase and helium nanodroplets. [27, 38] Despite rather weak interaction with He atoms, the He atoms in the innermost shell bind tightly with the cations,

causing the change of the effective rotational constants. The rotational constant *A* for the rotation about the C_3 axis in He is found to be ~15% smaller than the B constant in the gas phase [38], where the *B* constant corresponds to the rotation about the C_3 axis. The rotational constant *B* for the rotation perpendicular to the C_3 axis is a factor of ~10^2 times smaller in He droplets as compared with the gas phase and could not be evaluated accurately. In the gas phase, the $^{12}CH_3^+$ and $^{13}CH_3^+$ cations are oblate symmetric top, whereas the spectra in helium nanodroplets are consistent with the prolate symmetric top. This switching effect is assigned to the tight binding of the two He atoms along the C_3 axis of the ions. [27]

In distinction to the spectrum of $^{12}CH_3^+$ measured previously in ref. [27], the spectrum in Fig. 4 was obtained with the He-filled collision cell. Therefore, the relative intensities of the sub-bands have an intensity ratio close to 1:2:1 as expected from the population ratio of the nuclear spin isomers in CH_3^+. In comparison the measurements in ref [27] were done without the collision cell, hence the liberation of cations from larger droplets required an absorption of multiple photons causing nonlinear dependence of the signal on the absorbance. Therefore intensity of the sub-bands in the ref [27] appear about a factor of three smaller than that of the central feature. The comparison of the intensities of the central features shows that the signal of $^{12}CH_3^+$ is approximately 100 times larger than that of $^{13}CH_3^+$. This agrees with the 1.3-1.8 % concentration of $^{13}CH_4$ in the CH_4 gas cylinder. The rotational constants and their comparison with the gas phase data for both cations are tabulated below.

Table 1: The comparison of rotational constants for $^{12}CH_3^+$ and $^{13}CH_3^+$ cations in the helium nanodroplets (HND) and the gas phase from ref [38].

	$^{12}CH_3^+$ in the gas phase	$^{13}CH_3^+$ in the gas phase	$^{12}CH_3^+$ in HND	$^{13}CH_3^+$ in HND
A	4.04*	4.09*	3.5	3.5
B	9.3*	9.3*	0.1	0.1
D_{KK}	0.005	0.005	0.06	0.075
ν	3107.9	3095.2	3127.8	3115.0

* Designation of the rotational constants as *A* and *B* is switched in free ions.

In both measurements in Fig 3a and 3b, the droplets were obtained at the same experimental conditions and should have a similar size distribution. Fig. 3 shows that the maximum of the CH_4^+ signal is achieved at a higher pickup pressure ($A = 1.3\times10^{-6}$ mbar) than that for the $^{13}CH_3^+$ signal ($A = 0.9\times10^{-6}$ mbar). The production of the $^{13}CH_3^+$ ions upon ionization of the methane molecules implies dissociative ionization with H atoms leaving the droplet. One would expect that the probability for the hydrogen atom to leave the droplet should decrease as the size of the droplets increases. In the larger droplets, the H-atoms may more readily lose kinetic energy and stay within the droplet leading to the formation of the CH_4^+ ions in addition to those produced directly via the ionization of the CH_4 molecules. Therefore, the higher probability for the formation of CH_3^+ in larger droplets is surprising. It is possible that CH_4^+ ions are also formed upon ionization of methane dimers. Small contribution from the dimers would lead to a small change in the overall shape of the pressure dependence curve in Fig. 3a and will mainly be manifested in the shift of the maximum of the curve towards higher pickup pressure.

Conclusions

We report infrared spectra of CH_4^+ cations in helium nanodroplets. The cations are generated by electron impact ionization of helium droplets doped with methane molecules. The spectra of the CH_4^+ are consistent with the C_{2v} global minimum structure, which is in agreement with previous calculations and experiments. No other isomer of the CH_4^+ cation could be observed in helium droplets.

Additionally, this work reports the infrared spectrum of $^{13}CH_3^+$ cations which have the same nominal m/z = 16 same as $^{12}CH_4^+$ ions. The $^{13}CH_3^+$ cation shows characteristics of a prolate symmetric top made up of two helium atoms tagged on the C_3 axis of the cation. The rotational constants A and D_{KK} for $^{13}CH_3^+$ are found to be 3.4 cm^{-1} and 0.06 cm^{-1}, respectively, the same as in the $^{12}CH_3^+$ isotopologues. In the case of $^{13}CH_3^+$ cations, the J-structure of the band could not be resolved indicating that the rotational constant B is smaller than ~0.1 cm^{-1}. In comparison to CH_3^+, the rotational structure in the spectra of the CH_4^+ cations could not be resolved, indicating at least a factor of three decrease in the rotational constants. The origin of this effect remains to be understood.

Acknowledgments

This work was supported by the NSF under Grant No. CHE-2102318 and CHE-2404883. The research stay of Sofia H. Allison at USC was supported by NSF REU under grant no. CHE-1757942 to the chemistry department of USC. The authors thank Paul Scheier for his comments on the possible involvement of the ^{13}C isotopes in this work. The authors acknowledge the contributions of Deepak Verma and Swetha Erukala at the early stages of this work.

References

[1] I. B. Bersuker, *The Jahn-Teller Effect* (Cambridge University Press, Cambridge, UK, 2006), The Jahn-Teller Effect, https://doi.org/10.1017/CBO9780511524769

[2] D. Opalka, and W. Domcke, *The Journal of Chemical Physics*, Interpolation of multi-sheeted multi-dimensional potential-energy surfaces via a linear optimization procedure. **138**, (22), 224103, (2013). https://doi.org/10.1063/1.4808358

[3] D. Opalka, and W. Domcke, *The Journal of Chemical Physics*, High-order expansion of $T_2 \times t_2$ Jahn–Teller potential-energy surfaces in tetrahedral molecules. **132**, (15), 154108, (2010). https://doi.org/10.1063/1.3382912

[4] U. Opik, and M. H. L. Pryce, *Proceedings of The Royal Society A*, Studies of the Jahn-Teller effect. I. A survey of the static problem. **238**, (1215), 425, (1957). https://doi.org/10.1098/rspa.1957.0010

[5] U. Jacovella, H. J. Worner, and F. Merkt, *Journal of Molecular Spectroscopy*, Jahn-Teller effect and large-amplitude motion in CH_4^+ studied by high-resolution photoelectron spectroscopy of CH_4. **343**, 62, (2018). http://dx.doi.org/10.1016/j.jms.2017.08.002

[6] H. J. Woerner, R. V. D. Veen, and F. Merkt, *Physical Review Letters*, Jahn-Teller Effect in the Methane Cation: Rovibronic Structure and the Geometric Phase. **97**, (17), 173003, (2006). https://doi.org/10.1103/PhysRevLett.97.173003

[7] T. Mondal, and A. J. C. Varandas, *The Journal of Chemical Physics*, Quadratic coupling treatment of the Jahn-Teller effect in the triply-degenerate electronic state of $CH_4^+CH_4^+$: Can one account for floppiness? **137**, (21), 214320, (2012). https://doi.org/10.1063/1.4768675

[8] T. Mondal, and A. J. C. Varandas, *The Journal of Chemical Physics*, The Jahn-Teller effect in the triply degenerate electronic state of methane radical cation. **135**, (17), 174304, (2011). https://doi.org/10.1063/1.3658641

[9] H. J. Woerner, X. Qian, and F. Merkt, *The Journal of Chemical Physics*, Jahn-Teller effect in tetrahedral symmetry: Large-amplitude tunneling motion and rovibronic structure of CH_4^+ and CD_4^+. **126**, (14), 144305, (2007). https://doi.org/10.1063/1.2712840

[10] M. N. Paddon-Row, D. J. Fox, J. A. Pople, K. N. Houk, and D. W. Pratt, *J. Am. Chem. Soc.*, Dynamic Jahn-Teller effect in methane radical cation. Location of the transition structures for hydrogen scrambling and inversion. **107**, (25), 7697, (1985). https://doi.org/10.1021/ja00311a078

[11] M. S. Reeves, and E. R. Davidson, *The Journal of Chemical Physics*, Potential surface symmetry and vibronic wave functions for methane cation. **95**, (9), 6551, (1991). https://doi.org/10.1063/1.461525

[12] A. W. Potts, and W. C. Price, *Proceedings of The Royal Society A*, Photoelectron spectra and valence shell orbital structures of groups V and VI hydrides. **326**, (1565), 181, (1972). https://doi.org/10.1098/rspa.1972.0004

[13] J. W. Rabalais, T. Bergmark, L. O. Werme, L. Karlsson, and K. Siegbahn, *Physica Scripta*, The Jahn-Teller Effect in the Electron Spectrum of Methane. **3**, (1), 13, (1971). https://iopscience.iop.org/article/10.1088/0031-8949/3/1/004

[14] R. Signorell, and F. Merkt, *Faraday Discussions*, PFI-ZEKE photoelectron spectra of the methane cation and the dynamic Jahn–Teller effect. **115**, 205, (2000). https://doi.org/10.1039/A909272B

[15] R. Signorell, and F. Merkt, *The Journal of Chemical Physics*, The first rotationally resolved spectrum of CH_4^+. **110**, (5), 2309, (1999). https://doi.org/10.1063/1.477965

[16] L. B. Knight Jr., J. Steadman, D. Feller, and E. R. Davidson, *J. Am. Chem. Soc.*, Experimental evidence for a C_{2v} ($^2B_1$) ground-state structure of the methane cation radical: ESR and ab initio CI investigations of methane cation radicals (CH_4^+ and $CD_2H_2^+$) in neon matrixes at 4 K. **106**, (12), 3700, (1984). https://doi.org/10.1021/ja00324a066

[17] L. B. Knight Jr., G. M. King, J. T. Petty, M. Matsushita, T. Momose, and T. Shida, *The Journal of Chemical Physics*, Electron spin resonance studies of the methane radical cations ($^{12,13}CH_4^+$, $^{12,13}CDH_3^+$, $^{12}CD_2H_2^+$,

$^{12}CD_3H^+$, $^{12}CD_4^+$) in solid neon matrices between 2.5 and 11 K: Analysis of tunneling. **103**, (9), 3377, (1995). https://doi.org/10.1063/1.470222
[18] R. Signorell, M. Sommavilla, and F. Merkt, *Chemical Physics Letters*, Jahn–Teller distortion in $CD_2H_2^+$ from a rotationally resolved photoelectron spectrum. **312**, (2-4), 139, (1999). https://doi.org/10.1016/S0009-2614(99)00949-5
[19] Z. Vager, T. Graber, E. P. Kanter, and D. Zajfman, *Physical Review Letters*, Direct observation of nuclear rearrangement in molecules. **70**, 3549, (1993). https://doi.org/10.1103/PhysRevLett.70.3549
[20] D. Kella, and Z. Vager, *The Journal of Chemical Physics*, A detailed study of conformations in the ground state of CH_4^+. **102**, (21), 8424, (1995). https://doi.org/10.1063/1.468833
[21] J. A. Davies, S. Yang, and A. M. Ellis, *Physical Chemistry Chemical Physics*, Infrared spectra of carbocations and CH_4^+ in helium. **23**, (48), 27449, (2021). https://doi.org/10.1039/D1CP03138D
[22] A. Iguchi, A. Singh, S. Bergmeister, A. A. Azhagesan, K. Mizuse, A. Fujii, H. Tanuma, A. Toshiyuki, P. Scheier, S. Kuma~~, and A. F. Vilesov~~et al., *The Journal of Physical Chemistry Letters*, Isolation and Infrared Spectroscopic Characterization of Hemibonded Water Dimer Cation in Superfluid Helium Nanodroplets. **14**, (36), 8199, (2023). https://doi.org/10.1021/acs.jpclett.3c02150
[23] C. J. Moon, S. Erukala, A. J. Feinberg, A. Singh, M. Y. Choi, and A. F. Vilesov, *The Journal of Chemical Physics*, Formation of the $C_4H_n^+$ (n = 2–5) ions upon ionization of acetylene clusters in helium droplets. **158**, (22), 2244307, (2023). https://doi.org/10.1063/5.0150700
[24] S. Erukala, A. J. Feinberg, A. Singh, and A. F. Vilesov, *The Journal of Chemical Physics*, Infrared spectroscopy of carbocations upon electron ionization of ethylene in helium nanodroplets. **155**, (8), 084306, (2021). https://doi.org/10.1063/5.0062171
[25] A. Singh, A. J. Feinberg, C. J. Moon, S. Erukala, P. Kumar, M. Y. Choi, S. Venkataramani, and A. F. Vilesov, *The Journal of Chemical Physics*, Infrared spectroscopy of isomers of $C_3H_4^+$ in superfluid helium droplets. **160**, (21), 214306, (2024). https://doi.org/10.1063/5.0206412
[26] A. Iguchi, A. Singh, S. Kuma, H. Tanuma, and T. Azuma, *Journal of Molecular Spectroscopy*, Vibrational spectroscopy of aniline cations and their H-loss cations in helium droplets. **401**, 111903, (2024). https://doi.org/10.1016/j.jms.2024.111903
[27] S. Erukala, D. Verma, and A. F. Vilesov, *The Journal of Physical Chemistry Letters*, Rotation of CH_3^+ cations in helium droplets. **12**, (21), 5105, (2021). https://doi.org/10.1021/acs.jpclett.1c01274
[28] A. Singh, S. Bergmeister, A. A. Azhagesan, P. Scheier, and A. F. Vilesov, *Review of Scientific Instruments*, Infrared spectroscopy of cations in helium nanodroplets. **94**, (9), 093002, (2023). https://doi.org/10.1063/5.0163390
[29] A. Singh, S. H. Allison, A. A. A. Azhagesan, D. Verma, and A. F. Vilesov, *The Journal of Physical Chemistry Letters*, Infrared Spectroscopy of CH_5^+ Cations in Helium Nanodroplets. **15**, (44), 10931, (2024). https://doi.org/10.1021/acs.jpclett.4c02614
[30] J. Gspann, and H. Vollmar, *The Journal of Chemical Physics*, Metastable excitations of large clusters of ^{3}He, ^{4}He, or Ne atoms. **73**, (4), 1657, (1980). https://doi.org/10.1063/1.440347
[31] A. Mauracher, O. Echt, A. M. Ellis, S. Yang, D. K. Bohme, J. Postler, A. Kaiser, S. Denifl, and P. Scheier, *Phys Rep*, Cold physics and chemistry: Collisions, ionization and reactions inside helium nanodroplets close to zero K. **751**, (2018). https://doi.org/10.1016/j.physrep.2018.05.001
[32] S. Denifl, F. Zappa, I. Maehr, A. Mauracher, M. Probst, J. Urban, P. Mach, A. Bacher, D. K. Bohme, O. Echt, ~~T. D. Maerk, and P. Scheier~~et al., *The Journal of Chemical Physics*, Ionization of doped helium nanodroplets: Complexes of with water clusters. **132**, (23), 234307, (2010). https://doi.org/10.1063/1.3436721
[33] M. Matsushita, T. Momose, T. Shida, and L. B. Knight Jr., *The Journal of Chemical Physics*, Group theoretical study of the radical cation of methane: The effect of tunneling motions on the hyperfine interaction. **103**, (9), 3367, (1995). https://doi.org/10.1063/1.470221
[34] R. F. Frey, and E. R. Davidson, *The Journal of Chemical Physics*, Potential energy surfaces of CH_4^+. **88**, (3), 1775, (1988). https://doi.org/10.1063/1.454101

[35] R. Signorell, and M. Sommavilla, *Journal of Electron Spectroscopy and Related Phenomena*, CH_4^+: a fluxional ion? **108**, (1-3), 169, (2000). https://doi.org/10.1016/S0368-2048(00)00126-2
[36] H. J. Worner, R. V. D. Veen, and F. Merkt, *Physical Review Letters*, Jahn-Teller Effect in the Methane Cation: Rovibronic Structure and the Geometric Phase. **97**, (17), 173003, (2006). https://doi.org/10.1103/PhysRevLett.97.173003
[37] H. Hoshina, D. Skvortsov, B. G. Sartakov, and A. F. Vilesov, *The Journal of Chemical Physics*, Rotation of methane and silane molecules in He droplets. **132**, (7), 074302, (2010). https://doi.org/10.1063/1.3313925
[38] M. W. Croften, M.-F. Jagod, B. D. Rehfuss, W. A. Kreiner, and T. Oka, *The Journal of Chemical Physics*, Infrared spectroscopy of carbo-ions. III. ν_3 band of methyl cation CH_3^+. **88**, (2), 666, (1988). https://doi.org/10.1063/1.454194

TOC

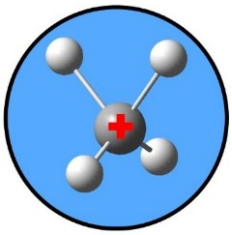

Copyright Disclaimer: This graphic has not been used elsewhere for publication.

Formatted: Justified